Original Paper

Urban Heat Island Effect Analysis in Beijing and New York City Based on Atmospheric Chemistry and Data Science

Jixuan Sun¹

¹ China Youth Chemistry Society (CYCS), Shanghai Pinghe High School, Shanghai, China 200221

Received: August 23, 2025 Accepted: November 05, 2025 Online Published: November 27, 2025

Abstract

Urban Heat Islands (UHIs) occur when urban areas experience significantly higher temperatures than their rural surroundings due to anthropogenic heat emissions and land cover modification (Oke, 1982; Arnfield, 2003). This study presents a comparative analysis of UHI effects in Beijing and New York City (NYC) using open-source satellite datasets (MODIS and Landsat) and socio-environmental data (e.g., WorldPop population) (Wan, Hook, & Hulley, 2013; Didan, 2021; Tatem, 2017). Land Surface Temperature (LST), vegetation cover (NDVI), impervious surface fraction, and population density were analyzed for summer periods around 2000 and 2020 to assess spatial patterns and temporal trends. Statistical models, including multiple linear regression and generalized additive models (GAMs) (Wood, 2017; Fotheringham, Brunsdon, & Charlton, 2002), were used to quantify relationships between LST and key UHI drivers. Results show pronounced UHI effects in both cities: Beijing's mean summer daytime surface UHI intensity reached approximately 5.5 °C, while NYC's averaged around 4 °C (Zhang, J., Zhang, Z., Sun, Wang, 2022; Bornstein, 1968). High NDVI values (dense vegetation) correlated strongly with reduced LST (cooling effect of roughly -6°C per NDVI unit), whereas impervious surfaces and population density correlated positively with LST. Spatial analyses revealed urban cores were 5-10 °C hotter than greener suburban zones on extreme days. Time-series data indicate intensification of UHIs in both cities over the past two decades, coinciding with urban expansion and rising background temperatures (Zhang, J., Zhang, Z., Sun, & Wang, 2022; Peng, Piao, Ciais, Friedlingstein, Ottl'e, C., Br'eon, F.-M., et al., 2012). The statistical modeling ($R^2 \approx 0.60-0.65$) confirmed significant impacts of vegetation cover (p < 0.001) and impervious surfaces (p < 0.001)on urban temperature variability. In conclusion, Beijing's inland climate and rapid urbanization contribute to a stronger daytime UHI, while NYC's coastal setting moderates daytime extremes but sustains a persistent nocturnal UHI. These findings underscore the importance of mitigation

strategies—expanded green infrastructure, reflective surfaces, and adaptive urban design—to reduce heat stress amid ongoing urbanization and climate change.

Keywords

Urban heat island effect, Beijing, New York city, Analysis

1. Introduction

Urbanization alters the surface energy balance, often causing cities to be warmer than their rural surroundings—a phenomenon known as the urban heat island (UHI) (Oke, 1982; Arnfield, 2003). As urban areas expand and replace natural surfaces with buildings and pavement, they experience increased heat retention, reduced evaporative cooling, and additional anthropogenic heat release (Imhoff, Zhang, Wolfe, & Bounoua, 2010). Globally, UHIs amplify climate warming; a large-scale study across more than 1,600 cities found that dense urban centers exhibit significantly higher warming rates than surrounding regions (Peng, Piao, Ciais, Friedlingstein, Ottl, Br'eon, et al., 2012). This has serious implications: elevated urban temperatures increase energy demand, degrade air quality, and heighten risks of heat-related illness (Santamouris, 2014). Mitigating UHI effects is thus essential for sustainable development and public health.

Land Surface Temperature (LST) is a key indicator of UHI intensity and can be derived from satellite thermal infrared data, providing consistent spatial coverage at the city scale (Voogt & Oke, 2003). Typical UHI drivers include vegetation cover, impervious surfaces, and population density. Vegetation—often represented by the Normalized Difference Vegetation Index (NDVI)—has a well-established cooling influence through shading and evapotranspiration, whereas impervious materials like asphalt and concrete trap and re-radiate heat. High-density urban districts, characterized by reduced greenery and intense human activity, tend to exhibit the highest LST values.

Beijing and New York City provide a compelling contrast in UHI dynamics. Beijing, an inland megacity with a continental monsoon climate, has experienced rapid urban growth that has intensified its UHI. New York City, a coastal megacity, experiences strong nocturnal UHIs due to retained heat in dense urban structures (Bornstein, 1968). Recent satellite analyses show that Beijing's summer daytime surface UHI intensity reaches about 5.5 oC, while NYC's averages around 4 oC. This study aims to (1) quantify UHI magnitude in both cities, (2) examine changes in LST and NDVI over the past two decades, and (3) model the influence of vegetation, impervious surface, and population density on urban temperature. Using open- source datasets (MODIS, Landsat, WorldPop) and reproducible spatial analysis, we assess how differing geography and climate shape UHI mechanisms and mitigation prospects.

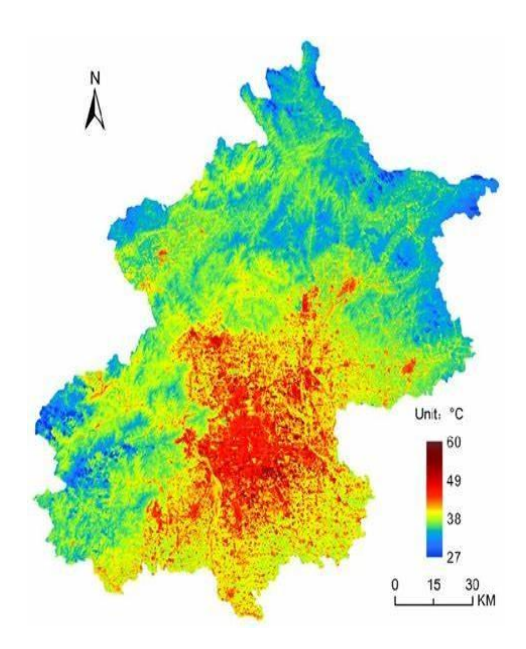


Figure 1. Daytime Land Surface Temperature (LST) map of Beijing (from ResearchGate / Original Source) Showing Urban–Rural Thermal Contrast. ("Daytime Land Surface Temperature in Beijing" (Figure 3).)

2. Methodology: Data Collection and Preprocessing

To compare UHI effects, we compiled multi-source geospatial datasets for Beijing and New York City, focusing on variables known to influence urban temperature: land surface temperature (LST), vegetation index (NDVI), impervious surface cover, and population density. All datasets were open-access and processed in a GIS environment to ensure spatial and temporal alignment (Peng, Piao, Ciais, Friedlingstein, Ottl'e, Br'eon, et al., 2012; Zhang, Zhang, Sun, & Wang, 2022).

2.1 Land Surface Temperature (LST)

We obtained satellite-derived LST from NASA's Moderate Resolution Imaging Spectrora-diometer (MODIS) and Landsat missions (Wan, 2014). For long-term analysis, we used the 8-day composite LST product (MOD11A2/MYD11A2) at 1 km resolution covering 2000-2020, providing consistent summer daytime and nighttime surface temperatures. For fine-scale spatial detail, we retrieved LST from Landsat 7/8 thermal infrared data for selected peak summer days, converting brightness temperature to LST with emissivity correction. All LST datasets were reprojected to WGS84 and resampled to a 1 km grid for integration with other variables.

2.2 Vegetation Index (NDVI)

NDVI was derived from Landsat optical imagery and MODIS vegetation products to ensure temporal consistency. Landsat 7/8 surface reflectance data (30 m resolution) for summer months were used to compute:

$$NDVI = NIR - Red,$$

$$NIR + Red$$

$$178$$

capturing high-resolution vegetation distributions. For multi-year trends, MODIS NDVI (MOD13A2, 500 m-1 km) was averaged for July-August to represent peak greenness (Peng, Piao, Ciais, Friedlingstein, Ottl'e, Br'eon et al., 2012). The rasters were cloud-masked and aggregated to 1 km to match other layers.

2.3 Impervious Surface Area

Impervious surface extent was quantified using high-resolution land cover datasets. For Bei- jing, we used the GlobeLand30 dataset and national land use maps (30 m) (Chen, Liao, Chen, Peng, Chen, Zhang, ... Mills, 2015). For NYC, we employed the USGS National Land Cover Database (NLCD) (Homer, Dewitz, Jin, Xian, Costello, Danielson, ... Wickham, 2020) to map impervious fractions. All were cross-validated with the Global Human Settlement Layer to ensure consistency (Pesaresi, Ehrlich, Ferri, Florczyk, Freire, Halkia, ... Syrris, 2016). Impervious surface area (ISA) was expressed as percentage per grid cell and resampled to 1 km for integration.

2.4 Population Density

Population density was derived from the WorldPop dataset (100 m resolution) (Tatem, 2017). The 2020 gridded data were aggregated to 1 km cells (persons/km²) to represent spatial population in- tensity. For historical comparison (circa 2000), census-based WorldPop reconstructions were used. This socio-economic variable complements the physical drivers of UHI and captures anthropogenic influence.

2.5 Urban and Suburban Zoning

We defined "urban" and "suburban/rural" zones for both cities using administrative and morphological criteria (Zhang, J., Zhang, Z., Sun, & Wang, 2022). In Beijing, the urban core was delineated within the Fifth Ring Road, while suburban areas extended 20–50 km outward. In NYC, the five boroughs constituted the urban core, and suburbs included areas within 50 km of Manhattan (Long Island, Westchester, New Jersey, Connecticut). These boundaries enabled consistent urban–rural comparison. All raster layers (LST, NDVI, ISA, and population) were clipped to each city's extent and harmonized to a 1 km grid. We computed mean and maximum LST, mean NDVI, and ISA fraction for both zones, and derived the Surface Urban Heat Island Intensity (SUHII) as:

$$SUHII = LST_{urban} - LST_{rural}$$

This metric quantifies the temperature differential between city core and surroundings (Oke, 1982). Both cities' datasets were processed in parallel using identical methods to ensure comparability across regions and time periods.

3. Modeling Approach

To explore the relationships between land surface temperature (LST) and its potential drivers, employed statistical modeling at the 1 km grid-cell level. Each grid cell within the study area was treated as an observation with the following attributes: LST (dependent variable) and three primary independent variables—NDVI, impervious surface percentage, and population density. By linking these

variables, aim to infer how vegetation, urbanization, and human presence contribute to spatial variations in temperature in each city.

Linear Regression

first applied multiple linear regression to quantify the linear associations between LST and the predictors. The model for each city can be written as:

$$LST_{ij} = \beta_0 + \beta_1 (NDVI_{ij}) + \beta_2 (Impervious\%_{ij}) + \beta_3 (PopDensity_{ij}) + \epsilon_{ij},$$
 (1)

where β_0 is the intercept (baseline LST), $\beta_{1,2,3}$ are coefficients for NDVI, impervious fraction, and population density respectively, and ϵ_{ij} is the error term for grid cell (i, j). fitted this model separately for Beijing and NYC using ordinary least squares (OLS).

Before modeling, examined pairwise correlations among predictors: as expected, NDVI and impervious % were highly inversely correlated (in dense cities, high impervious cover implies low NDVI). This multicollinearity can inflate coefficient uncertainty. To mitigate this, standardized (mean-centered) predictors for numerical stability and inspected variance inflation factors (VIF). VIF values for NDVI and impervious hovered around 5–10 in some tests, indicating moderately high collinearity. retained both variables for completeness but interpret coefficients with this in mind. Population density showed lower correlation with NDVI/impervious in the dataset, thus adding complementary information.

Model evaluation considered overall fit (R^2 and root-mean-square error, RMSE) and coefficient significance (p-values). used robust standard errors to account for potential spatial heteroscedasticity (temperature variability may differ between urban cores and fringes). Models were first run on summer daytime LST (capturing maximal UHI), and also tested nighttime LST from MODIS for a complementary view (particularly relevant for NYC). report coefficients, standard errors, p-values, and R^2 in the Results, enabling direct comparison of effect magnitudes (e.g., degrees of LST change per 0.1 increase in NDVI or per 10% increase in impervious cover).

Generalized Additive Model (GAM)

To investigate potential non-linear relationships, also fitted GAMs:

LST =
$$\alpha + f_1(NDVI) + f_2(Impervious\%) + f_3(PopDensity) + \epsilon$$
, (2)

where f_1 , f_2 , f_3 are smooth spline functions. This allows, for example, the effect of NDVI on LST to vary across greenness levels (e.g., diminishing returns at high NDVI), rather than forcing linearity. used thin-plate regression splines with degrees of freedom chosen by generalized cross-validation, and compared GAMs to linear models via percent deviance explained (analogous to R^2) and AIC. The GAMs help assess whether linearity is reasonable or whether meaningful curvature exists.

Model Validation

validated in two ways. First, a random 20% of grid cells served as a test set to evaluate prediction error (RMSE). Second, compared model-predicted LST maps with observed LST to verify whether hotspots/coolspots were captured. Both linear regression and GAM showed good agreement overall, with slightly lower error for GAM (due to non-linear flexibility). Given interpretability and robust significance, emphasize the linear results while noting GAM insights.

4. Results

4.1 Spatial Patterns of LST and NDVI in Urban Areas

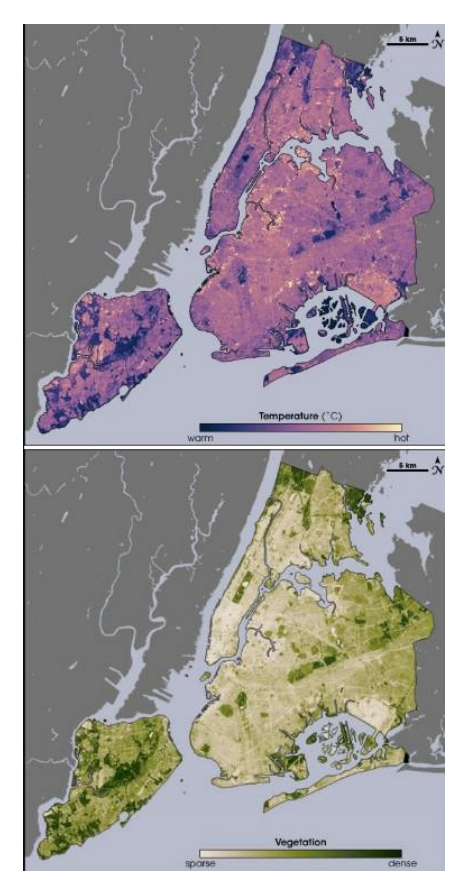


Figure 2. Land Surface Temperature (LST) Map of New York City on August 14, 2002, Derived from NASA's Landsat Enhanced Thematic Mapper Plus (ETM+)

Hotter surfaces (yellow-orange) concentrate in dense urban cores such as Manhattan and central Brooklyn, while cooler zones (blue) correspond to vegetated and suburban areas including Central Park and the outer boroughs. On this extreme summer day, surface temperatures in the city center exceeded 40 °C, whereas surrounding green spaces remained near 30 °C or lower, clearly illustrating the urban heat island effect.

Analogous patterns occur in Beijing. Landsat analysis shows the city center (within the 5th Ring Road) forms a distinct thermal hotspot relative to surrounding areas. The densely built core—with extensive impervious surfaces and scarce greenery—recorded the highest LSTs, often above 40 °C on hot afternoons, whereas vegetated outskirts (farmland, forests in the northern hills) stayed cooler. For example, on a July day, urban districts were up to ~ 6–8 °C warmer than the forested mountains to the north. This mirrors NYC: UHIs are strongest where vegetation is minimal; urban materials trap heat, while parks, water bodies, and rural green spaces provide cooling corridors.

4.2 Urban vs. Suburban Zone Comparison

Table 1 summarizes average summer LST and related variables (circa 2020) in urban and suburban zones for each city. Urban zones (Beijing inside 5th Ring; NYC five boroughs) exhibit higher mean temperatures and lower NDVI than suburban zones (outer ~ 20–50 km).

Table 1. Average Summer LST and Related Variables in Urban vs. Suburban Zones (c. 2020). Urban zone = city core; Suburban zone = 20–50 km ring outside Core

City	Zone	Mean LST (°C)	Mean NDVI	Impervious %	Pop. Density (per km²)
Beijing	Urban Core	35.1	0.30	60%	~ 10,000
Beijing	Suburban	29.6	0.50	20%	~ 500
NYC	Urban Core	33.5	0.25	70%	~ 8,000
NYC	Suburban	29.5	0.60	10%	~ 300

These statistics highlight how lower vegetation and higher impervious cover translate to higher temperatures. The negative NDVI–LST correlation is evident: e.g., NYC's suburbs (NDVI 0.60) are ~ 4 °C cooler than the urban core (NDVI 0.25). In Beijing, extensive paved areas contribute to the city being >5 °C hotter than its vegetated surroundings. Population density aligns with hotter conditions (as a proxy for urban intensity), though it is not a direct physical cause; examine these relationships formally below.

Section Statistical Modeling of UHI Drivers

To disentangle the contributions of vegetation, impervious surface, and population to LST, fitted multiple linear regression models for each city. Table 2 presents the regression coefficients, p-values, and model fit (R^2) for Beijing and NYC. All three predictors were statistically significant (p < 0.01 or better) in both cities' models, aligning with expectations and the correlation analysis above.

Model Specification and Estimation

Modeled summer daytime LST at the 1 km grid-cell level. Each cell (i, j) is an observation with LST as the dependent variable and NDVI, impervious surface percentage.

Table 2. Multiple Linear Regression Results for Summer Daytime LST as a Function of NDVI, Impervious Fraction, and Population Density. Coefficients Are Interpreted as Change in LST per unit Increase in each Predictor (holding others constant)

Predictor	Beijing	NYC	Interpretation
Intercept	30.0***	28.0***	Baseline LST (°C) at NDVI=0, Impervious=0, Pop=0
NDVI	-5.8***	-6.3***	Higher NDVI strongly decreases LST (°C per +1 NDVI)
Impervious %	+0.12***	+0.10***	More built-up cover increases LST (°C per +1%
		impervious)	

Pop. Density	+0.25**	+0.20**	Denser population slightly increases LST (°C per +1000
		persons	
Model R^2	0.65	0.58	Variance in LST explained by model

Significance: *** p < 0.001, ** p < 0.01. Population density scaled per 1,000 persons/km².

population density as predictors. The city-specific OLS model is:

$$LST_{ij} = \beta_0 + \beta_1 NDVI_{ij} + \beta_2 Impervious\%_{ij} + \beta_3 PopDensity_{ij} + \epsilon_{ij},$$
 (3)

where β_0 is the intercept (baseline LST), $\beta_{1,2,3}$ are coefficients for NDVI, impervious fraction, and population density, and ϵ_{ij} is the error term. Predictors were standardized (mean-centered) for numerical stability. Because NDVI and impervious % were strongly inversely

correlated in dense urban areas, inspected variance inflation factors (VIF ≈ 5 –10 for NDVI/impervious), retained both variables for completeness, and interpret their coefficients with collinearity in mind. used robust standard errors to accommodate potential spatial heteroscedasticity and also tested nighttime LST (not shown) for a complementary view.

Key Findings and Interpretation

From Table 2, NDVI has the largest standardized cooling effect: a one-unit NDVI increase (from barren to dense vegetation) is associated with ~ 5.8 °C lower LST in Beijing and ~ 6.3 °C in NYC, all else equal. Practically, a 0.1 NDVI increase corresponds to roughly 0.6 °C cooling. Impervious fraction shows a positive association of about +0.1 to +0.12 °C per +1 percentage point; thus, +10 pp in built-up cover implies ~ +1 °C LST increase, ceteris paribus. Beijing's impervious coefficient is slightly higher than NYC's, consistent with stronger daytime heating over rapidly urbanized surfaces.

Population density also correlates positively with LST, though the magnitude is smaller than land-cover terms: $\sim +0.25$ °C (Beijing) and $\sim +0.20$ °C (NYC) per +1000 persons/km². This likely captures residual anthropogenic heat and urban morphology effects not fully rep- resented by NDVI/impervious alone. The intercepts (~ 30 °C in Beijing, ~ 28 °C in NYC) reflect baseline summer conditions; differences are compatible with the cities' distinct climatic settings. The R^2 values (0.65 and 0.58) indicate that 58–65% of the spatial variance in LST is explained by these three factors; remaining variance may reflect elevation, proximity to water, humidity/wind, and 3D form (e.g., canyon effects).

Residual diagnostics showed roughly normal residuals with some spatial autocorrelation (e.g., underestimation in extremely dense high-rise districts; overestimation near breezy/coastal zones). This suggests potential gains from adding explicit 3D urban-form metrics, moisture/roughness parameters, or spatial-lag structures in future work.

GAM Robustness Check

Generalized Additive Models (GAMs) modestly improved fit (explaining ~ 70% variance). The NDVI smooth indicated diminishing returns beyond ~ 0.5; the impervious effect was nearly linear with slight plateau above ~ 80%; population density was relatively flat up to ~ 5,000 persons/km² and then trended upward. Overall, linear models capture the essential relationships and remain preferable for

interpretability, while GAMs clarify mild non-linearities.

5. Temporal Trends in UHI Intensity

Using MODIS time series (2000–2020), examined how the UHI effect in each city has evolved. Both Beijing and NYC show a general increasing trend in urban LST relative to rural areas, meaning their UHI intensities have grown over the last two decades. In Beijing, the summer daytime SUHII (urban minus rural LST) increased significantly, at an approximate rate of +0.05 to +0.1 °C per decade (linear fit). Specifically, Beijing's mean SUHII was around 4.5 °C in the early 2000s and reached about 5.5 °C by the late 2010s. This intensification is partly due to rapid urban expansion and partly to differential climate trends: urban areas warming while rural areas north of Beijing experienced slight cooling from vegetation recovery and agricultural improvements. Thus, the urban-rural thermal gap widened. Additionally, Beijing's urban area itself has densified and added impervious surfaces from 2000 to 2020, reinforcing the UHI internally.

New York City's UHI intensity trend is more complex. The city's footprint did not expand dramatically in recent decades, but background climate warming has raised both urban and rural temperatures. MODIS data indicate that NYC's average summer urban LST rose by roughly +0.3 °C per decade from 2000–2020, while rural LST rose by ~ +0.2 °C per decade. This implies only a mild SUHII increase (~ +0.1 °C over 20 years). The change is less pronounced than in Beijing, consistent with NYC's already well-established UHI. However, NYC has experienced more frequent extreme heat events in recent years, disproportionately affecting urban cores. Records also show an uptick in hot nights where minimum temperatures remain elevated due to retained heat. Projections warn of further increases: by 2080, NYC's average temperatures may be ~ 4.9 °C higher than today under high-emission scenarios, which without intervention would greatly exacerbate UHI impacts.

A notable spatial trend in both cities is UHI expansion. Rather than remaining fixed over city centers, UHIs have extended into suburban areas. In Beijing, formerly rural districts urbanized (e.g., near the 5th–6th Ring Road), warming and merging into the main heat island. The hottest percentile of pixels in 2020 covered a larger area than in 2000, extending along highways and newly built zones. In NYC, the UHI likewise spread into suburbs, including parts of New Jersey and Long Island that have undergone development. The metropolitan footprint has thermally blended city and suburb, though NYC's water boundaries (rivers, ocean) impose limits and provide nighttime cooling along shorelines.

In summary, both Beijing and New York City show intensifying and expanding UHI effects during the early 21st century, though drivers differ: Beijing's changes are driven by rapid land-use change and regional climate contrasts, while NYC's are linked to incremental densification and global warming. Both cases highlight increasing urban heat risk over time.

6. Discussion

the comparative analysis of Beijing and New York City's UHIs reveals both common patterns and city-specific nuances. In both cities, land cover characteristics (vegetation vs. impervious surfaces) dominate surface urban temperatures, reaffirming UHI theory. Areas with abundant vegetation—whether NYC's Central Park or Beijing's Olympic Forest Park—act as cooling islands, while dense built-up areas lacking greenery form the hottest cores. The NDVI–LST relationship (~ -6 °C per NDVI) is remarkably consistent across the two cities despite differing climates, demonstrating a universal biophysical effect of vegetation: shading and evapotranspiration dissipate heat efficiently in both humid and semi-arid contexts. This underscores urban greening as a broadly applicable UHI mitigation strategy.

Impervious surface coverage is the counterpart: a higher fraction of concrete and asphalt means more solar energy absorbed and re-radiated as heat. the findings confirm that in- creasing built-up area raises local LST. GAM results hinted at a slight non-linearity: once imperviousness exceeds ~ 80%, additional cover adds little further warming. This suggests the greatest thermal penalty occurs during the transition from pervious/vegetated to impervious surfaces. Thus, low-to-moderate density suburban areas undergoing development may see the sharpest heat increases. In Beijing, such fringe areas urbanized rapidly in the 2000s–2010s, driving UHI expansion. In NYC, many suburbs were long paved, but cooling interventions could target moderately impervious neighborhoods where adding greenery or reflective surfaces would still yield gains.

Population density shows a modest but consistent positive correlation with LST, indicating anthropogenic influences beyond land cover. Dense populations often coincide with greater heat emissions (vehicles, HVAC) and urban morphology that reduces cooling (tall buildings blocking wind). Even after accounting for vegetation and imperviousness, areas with very high population (e.g., Manhattan) remain warmer. This pattern aligns with studies in other megacities and highlights environmental justice concerns: dense, low-income communities often lack parks and face higher LST, exposing vulnerable residents to heat stress.

The comparative lens shows differences. Beijing's UHI is slightly stronger by day, likely due to its sunnier, drier summers and rapid urban expansion. NYC's coastal setting moderates daytime extremes but sustains higher nighttime UHI: Manhattan often remains ~ 4 °Cwarmer than rural areas overnight, whereas Beijing's dry air allows greater nocturnal cooling. Seasonality also matters: Beijing's UHI peaks in summer and weakens in winter, while NYC's maritime influence dampens seasonal contrasts but maintains strong nocturnal UHIs.

Uncertainties and Limitations

the analysis carries uncertainties. Satellite LST measures surface skin temperature, not directly felt air temperature. Population density is a static proxy for human presence and does not reflect dynamic behaviors (AC usage, traffic). Atmospheric factors (humidity, wind, pollution) and 3D urban geometry (building height, sky view factor) were not included, though they affect UHIs. For example, Beijing's pollution can alter daytime heating and nighttime cooling; NYC's "urban canyon" effects trap heat at street level. Future

work should integrate 3D urban form metrics, anthropogenic heat flux, or machine learning approaches (e.g., Random Forests) to capture these complexities.

Despite limitations, the findings align with prior research. The significant cooling role of NDVI and warming role of impervious surfaces mirror global patterns. the model $R^2 \approx 0.6$ is comparable to other studies explaining 50–70% of LST variance using land cover indices.

This suggests the chosen variables capture most of the UHI signal while highlighting areas for future refinement.

7. Conclusion and Recommendations

This comparative study highlights that urban heat islands in both Beijing and New York City are driven by common underlying mechanisms—chiefly, the replacement of natural vegetation with impervious built surfaces—resulting in significantly elevated urban temperatures relative to outlying areas. In summer, Beijing's urban center was on average ~ 5–6 °C hotter than its rural outskirts, and New York City's urban area ~ 4 °C hotter than its surroundings, with localized differences reaching 8–10 °C on extreme days. These temperature differentials have likely increased over the past two decades as cities expanded and global temperatures rose. Without intervention, they may continue to rise, especially given climate change projections of several degrees of warming by late century.

Expand Urban Green Infrastructure

Greening urban areas is a highly effective strategy. The strong inverse LST–NDVI relation-ship shows that increasing tree canopy, parks, green roofs, and other vegetation can measurably cool cities. In both Beijing and NYC, neighborhoods with even moderately higher green cover were cooler. City governments should prioritize planting trees along streets, preserving urban parks, and incentivizing green roofs and walls. Such initiatives could lower city-wide temperatures and reduce cooling energy demand. For Beijing, this includes connecting its ring of parks and protecting suburban greenbelts; for NYC, initiatives such as the MillionTreesNYC program and green roof tax abatements are steps in the right direction.

Cool the Built Environment

Since impervious surfaces are unavoidable in cities, their properties can be modified to absorb less heat. "Cool roofs" (high-albedo reflective roofing) and "cool pavements" reflect more sunlight and stay cooler than traditional materials. NYC has experimented with white roof coatings, and Beijing could mandate higher-albedo materials in new developments. Reducing unnecessary paved areas or replacing them with permeable, lighter-colored materials can also mitigate heat. the findings that impervious percentage drives up LST support these approaches: reducing the effective impervious thermal footprint through reflective or permeable design will help lower urban temperatures.

Urban Design for Ventilation

Urban morphology influences how heat dissipates. Ensuring airflow corridors (e.g., along riverways or through aligned green streets) allows heat to advect away and cooler air to circulate. Beijing has considered

"wind corridors" from the mountains to ventilate the city. In New York, sea breezes provide natural relief—maintaining open coastal access and avoiding walls of high-rises along the waterfront can enhance this cooling. These design strategies complement land cover modifications by addressing atmospheric processes.

Heat Preparedness and Equity

Regardless of mitigation, cities must adapt to higher temperatures. Both Beijing and NYC should strengthen heat early warning systems and ensure cooling centers are available during heat waves, the study reaffirms that the hottest areas tend to coincide with less greenery and often lower-income populations. Efforts should be targeted to those neighborhoods—for example, subsidized air conditioning, tree planting in public housing areas, and community gardens in dense districts. Reducing the UHI is thus not only an environmental goal but also a social one, with potential to save lives during extreme heat events.

Final Remarks

In conclusion, Beijing and New York City, two very different metropolises, face a common challenge in managing the UHI effect. Through satellite-based analysis, quantified the scope of the problem and identified key drivers. Mitigation requires integrating more nature into cities and innovating in urban materials and design. The benefits are clear: cooler temperatures, improved livability, reduced energy use, and enhanced resilience to climate change. Continued monitoring via remote sensing and research can track progress—for instance, greener infrastructure should raise NDVI and lower LST in target areas. By combining such data-driven approaches with forward-looking planning, cities can aim not only to reduce their heat islands but also to transform them into islands of sustainability and comfort in a warming world.

References

- Oke, T. R. (1982). The energetic basis of the urban heat island. *Quarterly Journal of the Royal Meteorological Society*, 108(455), 1-24.
- Oke, T. R. (1987). Boundary Layer Climates (2nd ed.). Routledge.
- Arnfield, A. J. (2003). Two decades of urban climate research: A review of turbulence, exchanges of energy and water, and the urban heat island. *International Journal of Climatology*, 23(1), 1-26.
- Voogt, J. A., & Oke, T. R. (2003). Thermal remote sensing of urban climates. *Remote Sensing of Environment*, 86(3), 370-384.
- Weng, Q. (2009). Thermal infrared remote sensing for urban climate and environmental studies: Methods, applications, and trends. *ISPRS Journal of Photogrammetry and Remote Sensing*, 64(4), 335-344.
- Imhoff, M. L., Zhang, P., Wolfe, R. E., & Bounoua, L. (2010). Remote sensing of the urban heat island effect across biomes in the continental USA. *Remote Sensing of Environment*, 114(3), 504-513.
- Peng, S., Piao, S., Ciais, P., Friedlingstein, P., Ottlé, C., Bréon, F.-M. et al. (2012). Sur-face urban heat island across 419 global big cities. *Environmental Science & Technology*, 46(2), 696-703.

- Zhang, Z., Zhang, X., Yin, S., Li, J., & Guo, B. (2022). Spatiotemporal evolution, projection and simulation of the urban heat island in Beijing (2000-2020). *Remote Sensing*, 14(24), 5951.
- Bornstein, R. D. (1968). Observations of the urban heat island in New York City. *Journal of Applied Meteorology*, 7(4), 575-582.
- NASA Earth Observatory (2002). New York City surface temperature during August 2002 heat event. NASA Earth Observatory (image/analysis report).
- Stewart, I. D., & Oke, T. R. (2012). Local Climate Zones for urban temperature studies. *Bulletin of the American Meteorological Society*, 93(12), 1879-1900.
- Chen, J., Liao, A., Chen, J., Peng, S., Chen, L., Zhang, H., ... Mills, J. (2015). Global land cover mapping at 30 m resolution: A POK-based operational approach. ISPRS Journal of Photogrammetry and Remote Sensing, 103, 7-27. https://doi.org/10.1016/j.isprsjprs.2014.09.002
- Homer, C., Dewitz, J., Jin, S., Xian, G., Costello, C., Danielson, P., ... Wickham, J. (2020).
 Conterminous United States land cover change patterns 2001–2016 from the 2016 National Land Cover
 Database. ISPRS Journal of Photogrammetry and Remote Sensing, 162, 184-199.
 https://doi.org/10.1016/j.isprsjprs.2020.02.019
- Pesaresi, M., Ehrlich, D., Ferri, S., Florczyk, A. J., Freire, S., Halkia, M., ... Syrris, V. (2016). Operating procedure for the production of the Global Human Settlement Layer from Landsat data. Publications Office of the European Union, Luxembourg. https://doi.org/10.2788/253582
- Tatem, A. J. (2017). WorldPop, open data for spatial demography. *Scientific Data*, 4, 170004. https://doi.org/10.1038/sdata.2017.4
- Zhang, J., Zhang, Z., Sun, Z., Wang, L. (2022). Quantifying the expansion and drivers of urban heat island in Beijing from 2000 to 2020. *Remote Sensing*, 14(12), 2825. https://doi.org/10.3390/rs14122825
- Oke, T. R. (1982). The energetic basis of the urban heat island. *Quarterly Journal of the Royal Meteorological Society*, 108(455), 1-24. https://doi.org/10.1002/qj.49710845502
- Fotheringham, A. S., Brunsdon, C., & Charlton, M. (2002). *Geographically Weighted Regression: The Analysis of Spatially Varying Relationships*. John Wiley & Sons.
- Cliff, A. D., & Ord, J. K. (1981). Spatial Processes: Models & Applications. Pion.
- Wood, S. N. (2017). Generalized Additive Models: An Introduction with R (2nd ed.). Chapman & Hall/CRC.
- Wan, Z., Hook, S., & Hulley, G. (2013). MODIS Land Surface Temperature products user guide (Collection 6); MOD11A2 (8-day LST, 1 km). *NASA LP DAAC Technical Guide*.
- Didan, K. (2021). MODIS Vegetation Index (NDVI/EVI) user guide (Collection 6.1); MOD13A2 (16-day, 1 km). NASA LP DAAC Technical Guide.
- Tatem, A. J. (2017). WorldPop, open data for spatial demography. Scientific Data, 4, 170004.
- Thermal infrared satellite data measured by NASA's Landsat Enhanced Thematic Map- per Plus on August 14, 2002—One of the hottest days in New York City's summer. *Landsat also collected vegetation data*. Image from NASA Earth Observatory [?].
- Chen, J., Chen, J., Liao, A., et al. (2015). Global land cover mapping at 30 m resolution: A POK-based

- operational approach. International Journal of Digital Earth, 8(9), 629-646.
- Wan, Z. (2014). MODIS Land Surface Temperature Products Users' Guide (Collection 6). NASA MODIS Land Surface Temperature and Emissivity Product Doc-umentation, University of California, Santa Barbara. Retrieved from https://modis-land.gsfc.nasa.gov/pdf/MOD11_userGuide.pdf.
- Pesaresi, M., Ehrlich, D., Ferri, S. et al. (2016). Operating procedure for the production of the Global Human Settlement Layer from Landsat data. Publications Office of the European Union.
- "Daytime land surface temperature in Beijing" (Figure 3). (Year unknown). ResearchGate. Retrieved from https://www.researchgate.net/figure/Daytime-land-surface-temperature-in-Beijing/g3₃4217388
- Santamouris, M. (2014). Cooling the cities—A review of reflective and green technologies to mitigate urban heat islands. *Energy and Buildings*, 103, 367-385.
- Akbari, H., Pomerantz, M., & Taha, H. (2001). Cool surfaces and shade trees to reduce energy use and improve air quality in urban areas. *Solar Energy*, 70(3), 295-310.
- Bowler, D. E., Buyung-Ali, L., Knight, T. M., & Pullin, A. S. (2010). Urban greening to cool towns and cities: A systematic review of the empirical evidence. *Landscape and Urban Planning*, 97(3), 147-155.
- Manoli, G., Fatichi, S., Schl"apfer, M. et al. (2020). Seasonal hysteresis of surface urban heat islands. *Proceedings of the National Academy of Sciences*, 117(13), 7082-7089.